AJNR

Prediction of Wound Failure in Patients with Head and Neck Cancer Treated with Free Flap Reconstruction: Utility of CT Perfusion and MR Perfusion in the Early Postoperative Period

Y. Ota, A.G. Moore, M.E. Spector, K. Casper, C. Stucken, K. Malloy, R. Lobo, A. Baba and A. Srinivasan

This information is current as of August 14, 2025.

AJNR Am J Neuroradiol published online 31 March 2022
http://www.ajnr.org/content/early/2022/03/31/ajnr.A7458

Published March 31, 2022 as 10.3174/ajnr.A7458

Prediction of Wound Failure in Patients with Head and Neck Cancer Treated with Free Flap Reconstruction: Utility of CT Perfusion and MR Perfusion in the Early Postoperative Period

Y. Ota, A.G. Moore, M.E. Spector, K. Casper, C. Stucken, K. Malloy, R. Lobo, A. Baba, and A. Srinivasan

ABSTRACT

BACKGROUND AND PURPOSE: Free flap reconstruction in patients with head and neck cancer carries a risk of postoperative complications, and radiologic predictive factors have been limited. The aim of this study was to assess the factors that predict free flap reconstruction failure using CT and MR perfusion.

MATERIALS AND METHODS: This single-center prospective study included 24 patients (mean age, 62.7 [SD, 9.0] years; 16 men) who had free flap reconstruction from January 2016 to May 2018. CT perfusion and dynamic contrast-enhanced MR imaging with conventional CT and MR imaging were performed between 2 and 4 days after the free flap surgery, and the wound assessments within 14 days after the surgery were conducted by the surgical team. The parameters of CT perfusion and dynamic contrast-enhanced MR imaging with conventional imaging findings and patient demographics were compared between the patients with successful free flap reconstruction and those with wound failure as appropriate. $P < .05$ was considered significant.

RESULTS: There were 19 patients with successful free flap reconstruction and no wound complications (mean age, 63.9 [SD, 9.5] years; 14 men), while 5 patients had wound failure (mean age, 58.0 [SD, 5.7] years; 2 men). Blood flow, blood volume, MTT, and time maximum intensity projection ($P = .007$, .007, .015, and .004, respectively) in CT perfusion, and fractional plasma volume, volume transfer constant, peak enhancement, and time to maximum enhancement ($P = .006$, .039, .004, and .04, respectively) in dynamic contrast-enhanced MR imaging were significantly different between the 2 groups.

CONCLUSIONS: CT perfusion and dynamic contrast-enhanced MR imaging are both promising imaging techniques to predict wound complications after head and neck free flap reconstruction.

ABBREVIATIONS: AIF = arterial input function; DCE = dynamic contrast-enhanced; EES = extravascular extracellular space; IQR = interquartile range; Kep = rate transfer constant between EES and blood plasma per minute; K^{trans} = volume transfer constant between EES and blood plasma per minute; SCC = squamous cell carcinoma; TME = time to maximum enhancement; tMIP = time maximum intensity projection; Ve = EES volume per unit tissue volume; Vp = fractional plasma volume

Head and neck cancer continues to carry a high risk of morbidity and mortality despite major advances in the fields of oncology and surgery.[1-3] One of the most impactful advances has been the ability to perform extensive surgical dissection followed by microvascular free tissue transfer.[4] Free flap viability with careful wound management is the key in the overall success of the procedure. Within the first 2 weeks after the operation, the flap is perfused solely by the anastomosed microvascular bed before endothelialization, inosculation of the anastomosis flap, and neoangiogenesis; thus, it is at highest risk for vascular thrombosis resulting in flap failure.[5] Multiple large studies have determined a combined 10%–40% risk of wound complications such as partial flap necrosis, wound breakdown, and fistula, with approximately 10% requiring surgical exploration in the setting of decreased viability.[6-8] Several studies have assessed the presurgical risk profile for the subsequent development of wound complications in head and neck free flaps such as diabetes, smoking history, preoperative radiation and chemotherapy history, and prolonged surgery time.[9-11]

A variety of techniques has been used to assess and monitor the perfusion of free flaps,[12] and Doppler ultrasound and skin paddle monitor have become the most popular methods. However, these

Received September 27, 2021; accepted after revision January 8, 2022.

From the Division of Neuroradiology (Y.O., R.L., A.B., A.S.), Department of Radiology, and Department of Otolaryngology (M.E.S., K.C., C.S., K.M.), University of Michigan, Ann Arbor, Michigan; and Department of Radiology (A.G.M.), Western Michigan University, Kalamazoo, Michigan.

This work received funding from the American Society of Head and Neck Radiology under the William N. Hanafee MD Research Grant and from the Internal Seed Grant of the Department of Radiology at the University of Michigan.

Please address correspondence to Ashok Srinivasan, MD, Division of Neuroradiology, Department of Radiology, B2-A209UH, University of Michigan, Michigan Medicine, 1500 E Medical Center Dr, Ann Arbor, MI, 48109; e-mail: ashoks@med.umich.edu

Indicates open access to non-subscribers at www.ajnr.org

Indicates article with online supplemental data.

http://dx.doi.org/10.3174/ajnr.A7458

Copyright 2022 by American Society of Neuroradiology.

methods assess only superficial vasculature and are not suitable for the assessment of the deep tissue vasculature. A single study assessed the role of CTA in the diagnosis of pedicle vascular stenosis in patients with head and neck microvascular free flap reconstruction and showed a sensitivity of 63% for detecting vascular pedicle stenosis.[13] While CTA can provide additional information for clinicians to use in the monitoring of flap viability, CTA cannot assess microperfusion alterations that play a crucial role in flap viability. During the early postoperative period when the flap vascularity is solely dependent on the microvascular anastomoses, noninvasive tissue-level perfusion imaging may provide predictive information for the development of wound failure and may also be used for risk-stratification and treatment protocols. The perfusion technique has been used for the assessment of microperfusion for disease differentiation and treatment-response prediction in the head and neck.[14-17] However, there are no studies in the literature using CT and MR perfusion for the assessment of head and neck free flap viability in the early postoperative period.

Our study was, therefore, designed to assess predictive factors for the development of wound complications in patients undergoing free flap reconstruction using CT and MR perfusion.

MATERIALS AND METHODS

The institutional review board of University of Michigan approved this prospective single-center research study, and informed consent for participation in this research was obtained from all participants. Data were acquired in compliance with all applicable Health Insurance Portability and Accountability Act regulations.

Study Population

We initially enrolled 38 patients at our institution from January 2016 to May 2018, according to the inclusion and exclusion criteria listed below.

Inclusion criteria were as follows:

1. Patients in the early postoperative period (days 2–4) following free flap reconstruction for head and neck malignancy, nonfunctional larynx, or other complications due to previous radiation therapy
2. Patients considered clinically at high risk for decreased tissue viability, defined as patients with a history of head and neck radiation
3. Patients who signed informed consent prior to imaging.

Exclusion criteria were as follows:

1. Patients who tested positive for pregnancy
2. Patients who were are younger than 18 years of age
3. Patients with contraindications to MRI due to noncompatible devices such as cardiac pacemakers, other implanted electronic devices, metallic prostheses, or ferromagnetic prostheses (eg, pins in artificial joints and surgical pins/clips)
4. Patients with contraindications to CT with IV contrast or to gadolinium administration.

Patient eligibility was confirmed with our inclusion and exclusion criteria, and patients were approached for enrollment in the study before their operation. While 38 patients consented before their operation, 14 patients dropped out of the study on the day of their scheduled scans. All patients were maintained in a reverse Trendelenburg position during the postoperative period in their recovery beds to help reduce facial and neck swelling; among the total 38 patients, the 14 patients who dropped out were unsure if they could lie flat for longer than 5 minutes to tolerate the CT perfusion and/or dynamic contrast-enhanced (DCE)-MR imaging scans. Therefore, the final inclusion in our study was 24 participants (mean age, 62.7 [SD, 9.0] years; 16 men) who had free flap reconstruction and postsurgery imaging.

Determination of Wound Failure

Patients were hospitalized following their operation at the discretion of the head and neck surgeon. The wound was examined twice per day by the surgical team, and the status of the wound was electronically recorded for documentation. Free flap viability was checked every hour for the first 24 hours, every 2 hours for the second 24 hours, every 4 hours for postoperative third-to-seventh day, and every 8 hours after the seventh postoperative day. The free flap was assessed by a variety of methods, including skin paddle evaluation when applicable and external Doppler ultrasound for the main anastomotic pedicle. The patients were discharged after confirmation of a general condition of stability and absence of wound complications. The patients returned to the outpatient clinic to have the wound checked 1 week after discharge.

Wound failure was assessed by the surgical team during the hospitalization period and at the first postoperative appointment. Wound failure was considered "positive" by the following definitions: total flap loss, partial flap loss, wound dehiscence (separation of skin edges), native skin breakdown, and the presence of a pharyngocutaneous fistula or the conditions requiring re-operation such as venous congestion and ecchymosis of a free flap.

Imaging Protocol

All imaging was obtained within 2–4 days following the operation during the inpatient admission phase.

CT Perfusion Protocol. Axial images were obtained on a 64-section MDCT scanner (HD750; GE Healthcare) following the administration of 75 mL of iopamidol injection (Isovue 300; Bracco) at a 5-mm section thickness, 40-mm z-axis coverage, 50-second scan duration, 5-second start delay, and 1-second delay between images. Conventional CT images at 1.25-mm section thickness were then obtained for the entire neck 35 seconds after the administration of an additional 75 mL of iopamidol.

DCE-MR Imaging Protocol. Following the acquisition of precontrast T1WI and T2WI through the ROI at 3-mm section thickness on a 3T magnet (Ingenia; Philips Healthcare), a DCE-MR imaging sequence was performed using 3D T1-weighted fast-field echo. The parameters of 3D T1 fast-field echo were as follows: TR = 4.6 ms; TE = 1.86 ms; flip angles = 5°, 10°, 15°, 20°, and 30°; section thickness = 2.5 mm; FOV = $240 \times 240\ mm^2$; voxel size = $1.0 \times 1.0 \times 5.0\ mm^3$; NEX = 1; number of slices per dynamic scan = 48; temporal resolution = 8.4 seconds; and total acquisition time = 4 minutes and 13 seconds, using a 16-channel Neurovascular Array Coil (Medrad) with the administration of gadobenate dimeglumine contrast (MultiHance; Bracco Diagnostics). An intravenous bolus of 20 mL of gadobenate

dimeglumine was administered using a power injector with a flow rate of 5.0 mL/s through a peripheral arm vein, followed by a 20-mL saline flush. These techniques were performed for all patients at a single center (University of Michigan).

The CT and MR imaging were both completed on the same day for all patients. The MR imaging was completed before the CT. While the entire free flap was covered on the DCE-MR imaging acquisition in the z-axis, only the central 4 cm demonstrating the region of anastomosis was covered on the CT perfusion acquisition. At the time of implementation of the study, we did not have the shuttle mode available on all the CT scanners running on the MDCT scanner platform at our institution, which could have increased our z-axis coverage to 8 cm. Hence, we elected to keep the z-axis coverage to the standard 4 cm on these research scans to avoid introducing more heterogeneity in the protocols.

Data Analysis

Patient Demographics. The patient demographics were reviewed from the electronic medical record and included the following information: age, sex, history of diabetes, history of chronic kidney disease, history of hypertension, body mass index, the original pathology and its staging, types of surgeries, history of radiation and chemotherapy, types of free flap, ischemia time (the time from disconnection of the free flap to the time to connect the flap to vessels in the neck), and wound infections.

Conventional Imaging Characteristics. All conventional CT and MR images were reviewed by a board-certified radiologist with 7 years of experience in neuroradiology and a board-certified otolaryngologist with 14 years of experience. They were aware of patients' demographics but blinded to whether the patients experienced postoperative complications. With consensus, they evaluated imaging characteristics using the following metrics:

1. Fluid collections in the postsurgical area, evaluated on CT and T2WI, recorded as binary variables (yes/no), and defined as a low-density area on CT and a hyperintense area on T2WI
2. Pedicle vascular structures within the free flap, evaluated on postcontrast CT, recorded as binary variables (yes/no), and defined as enhanced linear or tortuous structures on postcontrast CT and T1WI. The presence of venous thrombosis was recorded if present and recognized.

CT Perfusion Analysis. All analyses in CT perfusion were performed using commercially available software (Olea Sphere, Version 3.0; Olea Medical). The radiologist with 7 years' experienced and the otolaryngologist with 14 years' experience manually placed 5 separate ROIs on postcontrast head and neck CT scans with consensus and transferred them to the perfusion maps. The ROIs were carefully placed in the junctional areas of the free flap in the head and neck, avoiding placement of the ROIs in fluid collections or in the areas where streak or other artifacts degraded the imaging quality. These were not restricted to 1 axial section, were based on the orientation of the flap, and covered 1–3 axial slices in all patients. The values of generated CT perfusion parameters (blood volume, blood flow, TTP, time-to-maximum, MTT, and time maximum intensity projection (tMIP) of the 5 ROIs were averaged. We had decided to measure 5 separate ROIs because of the need to identify different areas of the free flap that may be affected differentially by perfusion abnormalities. An arterial input function (AIF) was calculated automatically using cluster analysis techniques, and deconvolution of the AIF was performed with a time-insensitive block-circulant singular-value decomposition.[18] While this process was automated, the corresponding density time curves that demonstrated a rapid increase in density with sharp peaks were deemed appropriate and accurate for analysis.

DCE-MR Imaging Analysis. All quantitative analyses in DCE-MR imaging were performed busing the OleaSphere 3.0 software permeability module, which is based on the extended Tofts model, by which pixel-based parameter maps are calculated from time-intensity curves. The radiologist with 7 years' experience and the otolaryngologist with 14 years' experience manually placed 5 separate ROIs on the conventional T1 postcontrast images and transferred them to the permeability maps with consensus. The ROIs were carefully placed in the junctional areas of the free flap in the head and neck, avoiding placement in fat tissues and fluid collections or in the areas where susceptibility artifacts from blood products or surgical clips degraded the imaging quality. Similar to the CT perfusion analysis, these were not restricted to 1 axial section, were based on the orientation of the flap, and covered 1–3 axial slices in all patients. The calculated quantitative parameters were fractional plasma volume (Vp), extravascular extracellular space (EES) volume per unit tissue volume (Ve), the volume transfer constant between EES and blood plasma per minute (K^{trans}), and the rate transfer constant between EES and blood plasma per minute (Kep).

Semiquantitative analysis was also performed using the same ROIs described above with the Olea Sphere 3.0 software permeability module. The averaged signal intensity within the ROIs was plotted against time, and time-intensity curves were constructed. The following parameters were calculated on a pixel-by-pixel basis from time-intensity curves: area under curve (the relative quantity of contrast agent across time), peak enhancement (maximum concentration of contrast agent), wash-in (velocity of enhancement), washout (velocity of enhancement loss), maximum signal-enhancement ratio, and time to maximum enhancement (TME). The values of DCE-MR imaging quantitative and semiquantitative parameters of the 5 ROIs were averaged. The AIF was individually computed, and AIF curves with a rapid increase in signal enhancement and a sharp peak followed by minimal temporal noises were chosen for DCE analysis. Representative cases of the group with successful flap reconstruction and the group with wound failure are shown in Figs 1 and 2.

Statistical Analysis

This cohort was divided into 2 groups: the group with successful free flap reconstruction (group I) and the group with any type of wound failure (group II, defined as total flap loss, partial flap loss, wound dehiscence [separation of skin edges], native skin breakdown, the presence of pharyngocutaneous fistula, or a condition that needed a re-operation such as venous congestion and ecchymosis of a free flap).

As for the patient demographics and conventional imaging characteristics, age was compared using an unpaired *t* test, and body mass index and ischemia time were compared using the

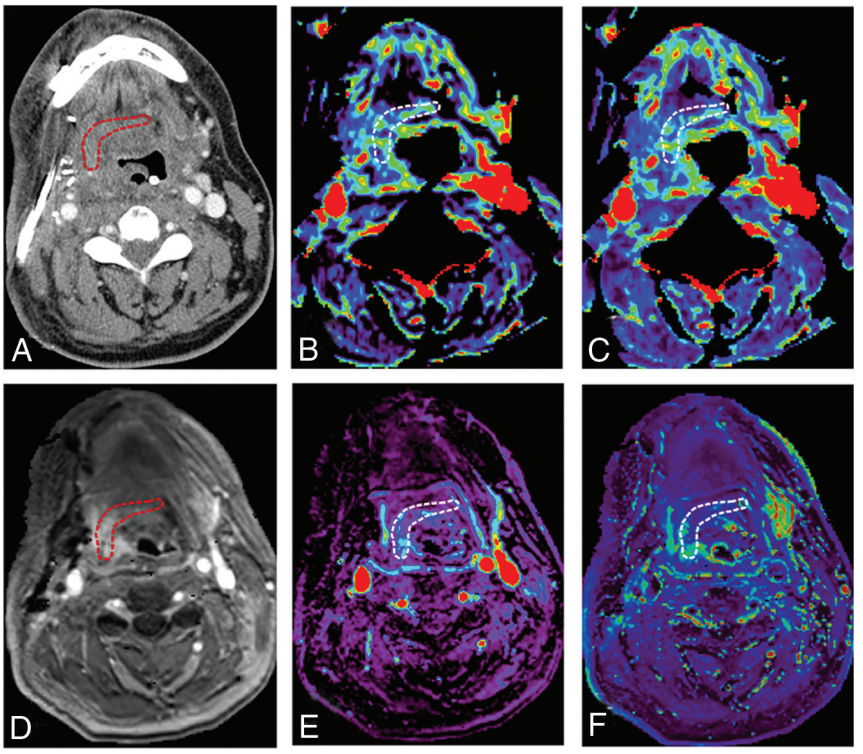

FIG 1. A 49-year-old male with tonsillar squamous cell carcinoma was treated with glossectomy, mandibulotomy, and neck dissection. An anterolateral thigh free flap was utilized for treatment of the soft tissue defect. No wound failure was observed. DCE-MR imaging and CT perfusion were performed 3 days after the surgery. *A*, An ROI is placed within the junctional area of the free flap on contrast enhanced CT. *B*, Blood volume (mL/100 ml) and *C*, blood flow (mL/100 ml/min) are calculated and are 7.67 mL/100 ml, 29.7 mL/100 ml/min, respectively. *D*, An ROI is placed on the permeability map within the junctional area of the free flap and DCE-MR imaging parameters are calculated. *E*, Vp and *F*, K^{trans} ($minute^{-1}$) are 0.17 and 0.19 ($minute^{-1}$), respectively. *Red* and *white circled areas* represent region of interests.

Mann-Whitney *U* test. Binary or categoric valuables such as sex, history of diabetes, history of chronic kidney disease, history of hypertension, history of radiation and chemotherapy therapy, the presence of wound infections, fluid collections in the postsurgical areas, and pedicle vascular structures were compared using the Fisher exact test between 2 groups.

As for CT perfusion parameters (blood volume, blood flow, TTP, time-to-maximum, MTT, and tMIP) and DCE-MR imaging parameters (Vp, Ve, K^{trans}, Kep, area under curve, peak enhancement, wash-in, washout, maximum signal-enhancement ratio, and TME), these were compared using the Mann-Whitney *U* test and are described as median (interquartile range [IQR]).

For values that showed statistically significant differences in CT perfusion parameters and DCE-MR imaging parameters, the optimal cutoff values in receiver operating characteristic analysis were determined as a value to maximize the Youden index (sensitivity + specificity −1). The diagnostic performances (sensitivity, specificity, positive predictive value, negative predictive value, and accuracy) were calculated on the basis of the cutoff values.

All statistical calculations were conducted with R statistical and computing software (Version 4.1.1; http://www.r-project.org) in this study. Variables with $P < .05$ were considered statistically significant.

RESULTS

Group I was composed of 19 patients (mean age, 63.9 [SD, 9.5] years; 14 men), and group II had 5 patients (mean age, 58.0 [SD, 5.7] years; 2 men). Group II consisted of 1 case of partial flap loss, 3 cases of pharyngocutaneous fistula, and 1 case of venous congestion and ecchymosis of a free flap with a reoperation.

The partial flap loss occurred 11 days after the operation; pharyngocutaneous fistula, 7, 9, and 10 days after the surgery; and venous congestion, 2 days after the surgery.

The types of free flap were anterolateral thigh free flaps (18/24), radial forearm free flap (1/24), latissimus dorsi free flap (2/24), gastro-omental free flap and split thickness skin graft (1/24), and scapula free flap with latissimus dorsi (2/24). Three anterolateral thigh free flaps and 2 scapula free flaps with the latissimus resulted in wound failure.

The original pathologies were all irradiated previously. The indications for free flap reconstruction were recurrence of the following pathologies or complications of radiation therapy: supraglottic squamous cell carcinoma (SCC) (7/24), recurrent glottic SCC (6/24), a nonfunctional larynx due to previous radiation therapy (4/24), osteoradionecrosis due to previous radiation therapy (1/24), pharyngocutaneous fistula due to previous radiation therapy (1/24), recurrent tongue SCC (1/24), recurrent hypopharyngeal SCC (1/24), recurrent tonsillar SCC (1/24), oral cavity SCC (1/24), and soft palate SCC (1/24).

There was no significant difference in numeric or categoric variables in the patient demographics between the 2 groups. The patient demographics are shown in the Online Supplemental Data and Table 1. For conventional imaging characteristics, there were no significant differences in fluid collections or pedicle vascular structures between the 2 groups ($P = .38$ and .14).

CT Perfusion

CT perfusion was performed at a median of 3 days after the operations (IQR, 2–4 days). Blood flow, blood volume, and tMIP were significantly higher in group I than group II (blood flow: median, 39.1 mL/100 mL/min [IQR, 27.9–45.6 mL/100 mL/min] versus 16.8 mL/100 mL/min [IQR, 14.0–17.1 mL/100 mL/min]; $P = .007$; blood volume: median, 7.67 mL/100 mL [IQR, 6.4–10.7 mL/100 mL] versus 4.58 mL/100 mL [IQR, 4.37–5.10 mL/100 mL]; $P = .007$; tMIP: median, 15.1 [IQR, 14.1–17.2] versus 6.78 [IQR, 4.81–8.74]; $P = .004$, respectively). MTT was significantly shorter in group I than in group II (MTT: median, 13.9 seconds [IQR, 12.9–15.6 seconds] versus 16.7 seconds [IQR, 16.5–17.0 seconds];

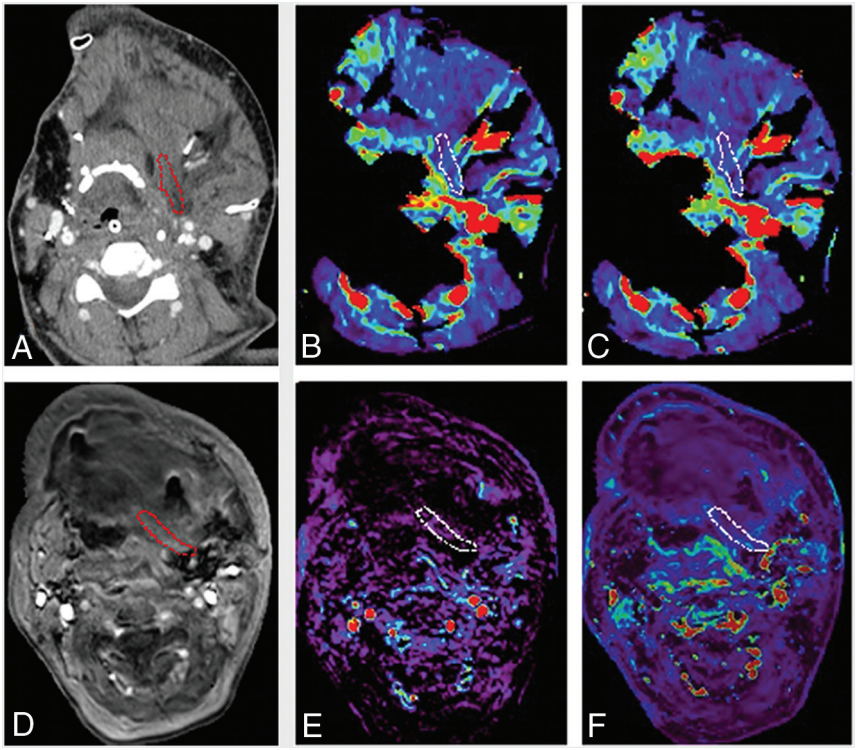

FIG 2. A 52-year-old woman with oral cavity squamous cell carcinoma was treated with mandibulectomy, glossectomy, tracheostomy, and neck dissection. A scapula free flap with latissimus dorsi was used to cover the soft tissue defect. The complication of venous congestion and ecchymosis was observed 2 days after the surgery. *A*, An ROI is placed within the junctional area of the free flap on contrast enhanced CT. *B*, Blood volume (mL/100 ml) and *C*, blood flow (mL/100 ml/min) are calculated and are 4.17 mL/100 ml and 11.3 mL/100 ml/min, respectively. *D*, An ROI is placed on the permeability map within the junctional area of the free flap and DCE-MR imaging parameters are calculated. *E*, Vp and *F*, K^{trans} (minute^{-1}) are 0.03 and 0.15 (minute^{-1}), respectively. *Red* and *white circled areas* represent region of interests.

Table 1: Demographic and imaging characteristics differences between the 2 groups[a]

	Group I	Group II	*P* Value
No. of patients	19	5	NA
Sex (male/female)	14:5	2:3	.29
Age (yr)	63.9 (SD, 9.5)	58.0 (SD, 5.7)	.20
BMI (kg/m^2)	24.1 (22.4–29.3)	21.1 (16.1–24.7)	.14
History of smoking	17/19	5/5	1
History of HT	4/19	2/5	.57
History of DM	1/19	2/5	.10
History of previous radiation	19/19	5/5	1
History of previous chemotherapy	13/19	4/5	1
Ischemia time (mins)	60 (45–95)	105 (90–109)	.34
Presence of wound infection	1/19	3/5	.10
Presence of fluid collection	7/19	1/5	.38
Presence of pedicle vascular structure	7/19	4/5 (Venous thrombosis: 1/5)	.14

Note:—NA indicates not applicable; BMI, body mass index; HT, hypertension; DM, diabetes mellitus.
[a] Groups I and II represent the group with successful free flap reconstruction and the group with wound failure, respectively. Values were described as mean (SD) or median (IQR).

flow, blood volume, MTT, and tMIP showed areas under the curve ranging from 0.96 to 0.98 between the 2 groups. The mean size of ROIs was 46.3 cm^2. Two patients in group I and 2 patients in group II were unable to undergo CT perfusion due to their inability to lie still for the examination.

MR Perfusion

DCE-MR imaging was performed at a median 3 days after the operations (IQR, 2–4 days). Vp, K^{trans}, and peak enhancement were higher in group I than in group II (Vp: median, 0.11 [IQR, 0.06–0.15] versus 0.03 [IQR, 0.026–0.04]; $P = .006$; K^{trans}: median, 0.21 minute^{-1} [IQR, 0.18–0.27 minute^{-1}] versus 0.15 minute^{-1} [IQR, 0.12–0.16 minute^{-1}]; $P = .039$; peak enhancement: median, 257 [IQR, 167–275] versus 79 [IQR, 76.6–90.7]; $P = .004$). TME was shorter in group I than in group II (TME: median, 102 seconds [IQR, 77.3–118 seconds] versus 143 seconds [IQR, 137–150 seconds]; $P = .04$). Ve, Kep, area under curve, wash-in, washout, and maximum signal-enhancement ratio were not significantly different (Ve: median, 0.37 [IQR, 0.27–0.53] versus 0.28 [IQR, 0.24–0.31]; $P = .35$; Kep: median, 0.56 [IQR, 0.46–0.74] versus 0.56 [IQR, 0.54–0.58]; $P = .97$; area under curve: 6.76×10^3 [IQR, $4.55–11.7 \times 10^3$] versus 4.76×10^3 [IQR, $4.48–4.80 \times 10^3$]; $P = .49$; wash-in: 0.99 [IQR, 0.36–2.60] versus 1.97 [IQR, 0.31–3.15]; $P = .78$; washout: median, 0.16 [IQR, 0.08–1.08] versus 0.65 [IQR, 0.63–3.25]; $P = .09$; maximum signal-enhancement ratio: median, 97.1 [76.1–141.5] versus 86.9 [74.1–87.5]; $P = .50$).

Vp, K^{trans}, peak enhancement, and TME showed the areas under the curve ranging from 0.81 to 0.92 between the 2 groups. The ROI mean size was 43.1 cm^2. Three patients in group I were unable to undergo MR perfusion due to their inability to lie still for the examination. A pulsed input pattern was observed in the AIF curves in all patients in CT perfusion and DCE-MR imaging. The diagnostic performances of CT perfusion and DCE-MR imaging parameters are shown in the Table 2 and Figs 3 and 4. The distribution of CT perfusion and DCE-MR imaging parameters is shown in the Online Supplemental Data.

$P = .015$). TTP and time-to-maximum were not significantly different (TTP: median, 32.3 seconds [IQR, 30.6–36.5 seconds] versus 32.6 seconds [IQR, 32.5–33.9 seconds]; $P = .84$; time-to-maximum: median, 7.39 seconds [IQR, 6.29–10.8 seconds] versus 9.04 seconds [IQR, 8.44–10.3 seconds]; $P = .42$). Blood

Table 2: Diagnostic performance of CT perfusion and DCE-MR imaging in the prediction of wound failure after head and neck free flap reconstruction

	Blood Flow (mL/100 mL/min)	Blood Volume (mL/100 mL)	MTT (Sec)	tMIP	Vp	K^{trans} (min^{-1})	Peak Enhancement	TME (Sec)
Cutoff	17.3	5.62	16.1	10.7	0.06	0.15	155	113
Sensitivity	1	1	1	1	1	0.80	1	1
Specificity	0.94	0.88	0.88	0.94	0.81	0.94	0.81	0.69
PPV	0.75	0.60	0.60	0.75	0.63	0.80	0.63	0.50
NPV	1	1	1	1	1	0.94	1	1
Accuracy	0.95	0.90	0.90	0.95	0.86	0.91	0.86	0.76
AUC	0.96	0.96	0.96	0.98	0.92	0.82	0.91	0.81

Note:—PPV indicates positive predictive value; NPV, negative predictive value; AUC, area under the curve.

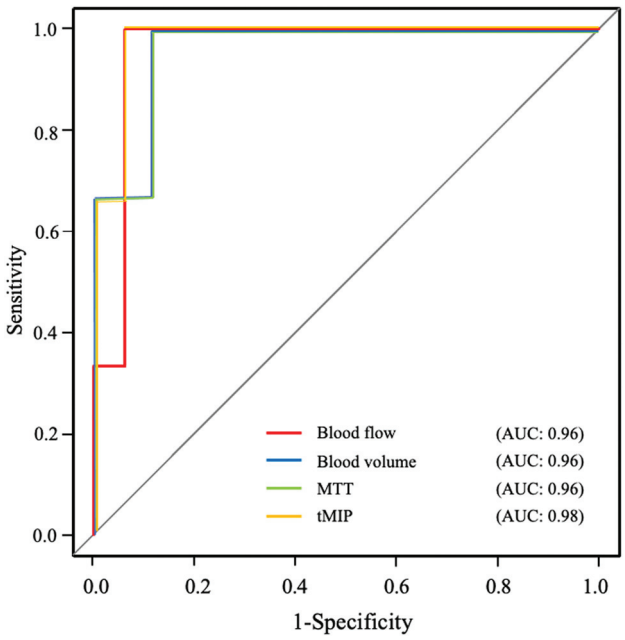

FIG 3. Receiver operating characteristic curves of CT perfusion parameters that showed statistically significant differences between groups I and II. AUC indicates area under the curve.

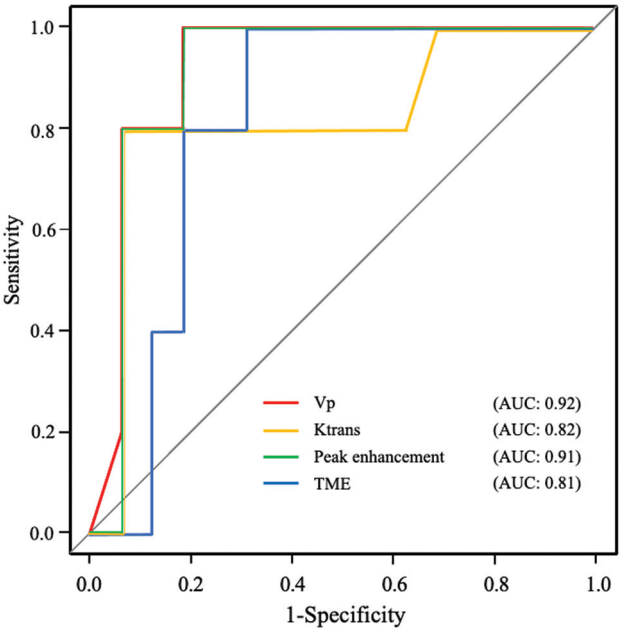

FIG 4. Receiver operating characteristic curves of DCE-MR imaging parameters that showed statistically significant differences between groups I and II. AUC indicates area under the curve.

DISCUSSION

Our study aimed to assess the utility of CT perfusion and DCE-MR imaging for predicting wound failure after free flap reconstructive head and neck surgery. While patient demographics and conventional imaging characteristics were unable to identify any differences between group I and group II, CT perfusion and DCE-MR imaging showed significant differences between the 2 groups in multiple parameters, with the receiver operating characteristics demonstrating diagnostic performances ranging from an area under the curve of 0.81 to 0.98. A direct comparison of the results from the 2 techniques was, however, not feasible due to the small sample size.

Prior studies have shown some risk factors related to wound failure such as a history of smoking, hypertension, elevated creatinine levels, wound infection, and chemoradiation therapy.[9-11] While the occurrence of wound failure was relatively high (5/24) in our study, none of the patient demographics or conventional imaging features related to the presence or absence of fluid collection and pedicle vascular structures were predictive of wound failure. In only 1 case with flap failure was there an identifiable venous thrombosis, which was thought to be the cause of the free flap ischemia.[19] This low detectivity of venous thrombosis in our cohort may be related to the difficulty in identifying venous thrombosis due to early timing of the CT/MR imaging acquisition and the relatively smaller venous outflow anatomy compared with the larger arterial pedicle. To maximize our chances of identifying advanced imaging-based parameters that could be helpful for the prediction of wound failure (and reduce the chances of having very few wound failures in our outcomes data set that would skew the results significantly), we had selected a group of patients who were considered at baseline as high risk for decreased tissue viability due to a prior history of chemoradiation (which causes chronic radiation-induced ischemia and has been identified as the most important determinant factor of wound failure).[10]

As for CT perfusion, blood flow, blood volume, and tMIP were significantly lower and MTT was longer in the group with wound failure (group II) than in the group with successful free flap reconstruction (group I). These results may suggest that the vasculature in the junctional areas within the free flap in the head and neck is less anastomosed and perfused in group II than in group I in the early postoperative stage (2–4 days). Regarding DCE-MR imaging

parameters, Vp and K^{trans} were significantly lower in group II than in group I. Similar to CT perfusion results, these may also indicate reduced microperfusion and permeability in group II. Moreover, TME and peak enhancement, which are based on the time-intensity curve and can represent local perfusion alterations, were also different between the 2 groups: Group II showed lower peak enhancement with a longer TME than group I. This finding is consistent with the results of Vp and K^{trans} and likely implies a prolonged transit of a smaller amount of contrast in hypoperfused free flaps.

One prior study using MR perfusion for postoperative monitoring showed an optimal detectivity of reduced blood flow after the operation in cutaneous, subcutaneous, and muscle tissue areas including 10 patients with tissue defects in various body regions.[20] Our study specifically focused on head and neck free flaps and was able to show the utility of both CT perfusion and MR perfusion in identifying an early postoperative hypoperfused state that may be a risk factor for wound failure. Together, these findings suggest that patients who have normal perfusion parameters on CT /MR imaging in the early postoperative period, as our study showed, may be candidates for early discharge from hospitalization or could return to a normal diet earlier than patients with abnormal parameters.

Our study has several limitations. While this study was prospective, it included only a relatively small population from a single institution, and some patients were unable to undergo CT or MR perfusion. However, even with the relatively small numbers, we were able to identify differences in CT and MR perfusion between the 2 groups studied. We were not able to compare the predictive performance between CT perfusion and DCE-MR imaging due to the small number of patients in this pilot study. Larger trials that incorporate more patients would be needed to study which of the 2 modalities (CT versus MR perfusion) is more robust and which of the parameters in each technique provides the best differentiation of the 2 groups. Second, we were unable to measure the perfusion in the entire free flap because a very large number or area of ROIs would be needed to cover all slices that contained the free flap. However, we mitigated this potential bias by focusing on the junctional area of the free flap that is most likely to fail after an operation and used 5 separate ROIs in all patients to cover as much of the junction as possible. Last, there was a significant dropout of patients from the study after enrollment due to their perceived inability to lie flat for the scans; this could be an impediment in routinely performing these scans for all postoperative patients, and some may require general anesthesia to tolerate the scans.

CONCLUSIONS

Parameters derived from CT perfusion and DCE-MR imaging can both serve as imaging biomarkers to predict wound complications after head and neck free flap reconstruction.

Disclosure forms provided by the authors are available with the full text and PDF of this article at www.ajnr.org.

REFERENCES

1. Wang Y, Wang M, Tang Y, et al. **Perioperative mortality of head and neck cancers.** *BMC Cancer* 2021;21:256 CrossRef Medline
2. Carvalho AL, Nishimoto IN, Califano JA, et al. **Trends in incidence and prognosis for head and neck cancer in the United States: a site-specific analysis of the SEER database.** *Int J Cancer* 2005;114:806–16 CrossRef Medline
3. Pulte D, Brenner H. **Changes in survival in head and neck cancers in the late 20th and early 21st century: a period analysis.** *Oncologist* 2010;15:994–1001 CrossRef Medline
4. Neligan PC. **Head and neck reconstruction.** *Plast Reconstr Surg* 2013;131:260e–69e CrossRef Medline
5. Yoon AP, Jones NF. **Critical time for neovascularization/angiogenesis to allow free flap survival after delayed postoperative anastomotic compromise without surgical intervention: a review of the literature.** *Microsurgery* 2016;36:604–12 CrossRef Medline
6. Simon C, Bulut C, Federspil PA, et al. **Assessment of peri- and postoperative complications and Karnofsky-performance status in head and neck cancer patients after radiation or chemoradiation that underwent surgery with regional or free-flap reconstruction for salvage, palliation, or to improve function.** *Radiat Oncol* 2011;6:109 CrossRef Medline
7. Bianchi B, Copelli C, Ferrari S, et al. **Free flaps: outcomes and complications in head and neck reconstructions.** *J Craniomaxillofac Surg* 2009;37:438–42 CrossRef Medline
8. Khouri RK, Cooley BC, Kunselman AR, et al. **A prospective study of microvascular free-flap surgery and outcome.** *Plast Reconstr Surg* 1998;102:711–21 CrossRef Medline
9. Lin PC, Kuo PJ, Kuo SCH, et al. **Risk factors associated with postoperative complications of free anterolateral thigh flap placement in patients with head and neck cancer: analysis of propensity score-matched cohorts.** *Microsurgery* 2020;40:538–44 CrossRef Medline
10. Furuta Y, Homma A, Oridate N, et al. **Surgical complications of salvage total laryngectomy following concurrent chemoradiotherapy.** *Int J Clin Oncol* 2008;13:521–27 CrossRef Medline
11. Sanati-Mehrizy P, Massenburg BB, Rozehnal JM, et al. **Risk factors leading to free flap failure: analysis from the national surgical quality improvement program database.** *J Craniofac Surg* 2016;27:1956–64 CrossRef Medline
12. Chao AH, Lamp S. **Current approaches to free flap monitoring.** *Plast Surg Nurs* 2014;34:52–56; quiz 57–58 CrossRef Medline
13. Abdel Razek AA, Denewer AT, Hegazy MA, et al. **Role of computed tomography angiography in the diagnosis of vascular stenosis in head and neck microvascular free flap reconstruction.** *Int J Oral Maxillofac Surg* 2014;43:811–15 CrossRef Medline
14. Gaddikeri S, Gaddikeri RS, Tailor T, et al. **Dynamic contrast-enhanced MR imaging in head and neck cancer: techniques and clinical applications.** *AJNR Am J Neuroradiol* 2016;37:588–95 CrossRef Medline
15. Ota Y, Liao E, Capizzano AA, et al. **Diagnostic role of diffusion-weighted and dynamic contrast-enhanced perfusion MR imaging in paragangliomas and schwannomas in the head and neck.** *AJNR Am J Neuroradiol* 2021;42:1839–46 CrossRef Medline
16. Ota Y, Liao E, Kurokawa R, et al. **Diffusion-weighted and dynamic contrast-enhanced MRI to assess radiation therapy response for head and neck paragangliomas.** *J Neuroimaging* 2021;31:1035–43 CrossRef Medline
17. Ota Y, Liao E, Capizzano AA, et al. **MR diffusion and dynamic-contrast enhanced imaging to distinguish meningioma, paraganglioma, and schwannoma in the cerebellopontine angle and jugular foramen.** *J Neuroimaging* 2021 Dec 22. [Epub ahead of print] CrossRef Medline
18. Mouridsen K, Christensen S, Gyldensted L, et al. **Automatic selection of arterial input function using cluster analysis.** *Magn Reson Med* 2006;55:524–31 CrossRef Medline
19. McCarty JL, Corey AS, El-Deiry MW, et al. **Imaging of surgical free flaps in head and neck reconstruction.** *AJNR Am J Neuroradiol* 2019;40:5–13 CrossRef Medline
20. Lamby P, Prantl L, Fellner C, et al. **Post-operative monitoring of tissue transfers: advantages using contrast enhanced ultrasound (CEUS) and contrast enhanced MRI (ceMRI) with dynamic perfusion analysis?** *Clin Hemorheol Microcirc* 2011;48:105–17 CrossRef Medline